EUROPEAN HEMATOLOGY ASSOCIATION
haematologica
Journal of the European Hematology Association

# Chronic sympathetic driven hypertension promotes atherosclerosis by enhancing hematopoiesis

by Annas Al-Sharea, Man K. S. Lee, Alexandra Whillas, Danielle Michell, Waled Shihata, Alyce J. Nicholls, Olivia D. Cooney, Michael J. Kraakman, Camilla Bertuzzo Veiga, Ann-Maree Jefferis, Kristy Jackson, Prabhakara R. Nagareddy, Gavin Lambert, Connie H. Y. Wong, Karen L. Andrews, Geoff A. Head, Jaye Chin-Dusting, and Andrew J. Murphy

Haematologica 2018 [Epub ahead of print]

*Citation: Annas Al-Sharea, Man K. S. Lee, Alexandra Whillas, Danielle Michell, Waled Shihata, Alyce J. Nicholls, Olivia D. Cooney, Michael J. Kraakman, Camilla Bertuzzo Veiga, Ann-Maree Jefferis, Kristy Jackson, Prabhakara R. Nagareddy, Gavin Lambert, Connie H. Y. Wong, Karen L. Andrews, Geoff A. Head, Jaye Chin-Dusting, and Andrew J. Murphy. Chronic sympathetic driven hypertension promotes atherosclerosis by enhancing hematopoiesis.*
*Haematologica. 2018; 103:xxx*
*doi:10.3324/haematol.2018.192898*

# Chronic sympathetic driven hypertension promotes atherosclerosis by enhancing hematopoiesis

Annas Al-Sharea[1]*, Man K. S Lee[1], Alexandra Whillas[1], Danielle Michell[1,2], Waled Shihata[1,3], Alyce J Nicholls[4], Olivia D Cooney[1], Michael J Kraakman[1,5], Camilla Bertuzzo Veiga[1], Ann-Maree Jefferis[3], Kristy Jackson[6], Prabhakara R Nagareddy[7], Gavin Lambert[8,9], Connie H. Y Wong[4], Karen L Andrews[3], Geoff A Head[6], Jaye Chin-Dusting[3], Andrew J Murphy[1,10]*

[1]Haematopoiesis and Leukocyte Biology Laboratory, Division of Immunometabolism, Baker Heart and Diabetes Institute, Melbourne, VIC, Australia.

[2]Department of Medicine, Vanderbilt University School of Medicine, Nashville, TN, USA.

[3]Department of Pharmacology, Monash University, Clayton, VIC, Australia.

[4]Centre for Inflammatory Diseases, Department of Medicine, Monash University, Clayton, VIC, Australia.

[5]Naomi Berrie Diabetes Center and Department of Medicine, Columbia University, New York, USA

[6]Neuropharmacology Laboratory, Division of Hypertension and Cardiac Disease, Baker Heart and Diabetes Institute, Melbourne, VIC, Australia.

[7]Department of Nutrition Sciences, University of Alabama at Birmingham, Birmingham, Alabama, USA

[8]Human Neurotransmitters Laboratory, Division of Hypertension and Cardiac Disease, Baker Heart and Diabetes Institute,

[9]Iverson Health Innovation Research Institute, Swinburne University of Technology, Hawthorn, VIC, Australia

[10]Department of Immunology, Monash University, Melbourne, VIC, Australia.

*Corresponding Authors

Associate Professor Andrew Murphy
Haematopoiesis and Leukocyte Biology
Baker Heart and Diabetes Institute
75 Commercial Road
Melbourne, Victoria, 3004.
Australia
Phone: +61 3 8532 1292
Email: andrew.murphy@baker.edu.au

Annas Al-Sharea
Haematopoiesis and Leukocyte Biology

Baker Heart and Diabetes Institute
75 Commercial Road
Melbourne, Victoria, 3004.
Australia
Phone: +61 3 8532 1429
Email: annas.al-sharea@bakeridi.edu.au

Running title – SNS driven hypertension enhances hematopoiesis

Keywords: Hematopoiesis, Hypertension, Sympathetic nervous system, Atherosclerosis.

Total word count: 7915

## Abstract

Hypertension is a major, independent risk factor for atherosclerotic cardiovascular disease. However, this pathology can arise through multiple pathways, which could influence vascular disease through distinct mechanisms. An overactive sympathetic nervous system is a dominant pathway that can precipitate in elevated blood pressure. We aimed to determine how the sympathetic nervous system directly promotes atherosclerosis in the setting of hypertension. We used a mouse model of sympathetic nervous system-driven hypertension on the atherosclerotic-prone apolipoprotein E deficient background. When mice were placed on a western type diet for 16 weeks we showed the evolution of unstable atherosclerotic lesions. Fortuitously, the changes in lesion composition were independent of endothelial dysfunction, allowing for the discovery of alternative mechanisms. With the use of flow cytometry and bone marrow imaging, we found that sympathetic activation caused deterioration of the hematopoietic stem and progenitor cell niche in the bone marrow, promoting the liberation of these cells into the circulation and extramedullary hematopoiesis in the spleen. Specifically, sympathetic activation reduced the abundance of key hematopoietic stem and progenitor cell niche cells, sinusoidal endothelial cells and osteoblasts. Additionally, sympathetic bone marrow activity prompted neutrophils to secrete proteases to cleave the hematopoietic stem and progenitor cell surface receptor CXCR4. All these effects could be reversed using the β-blocker propranolol during the feeding period. These findings suggest that elevated blood pressure driven by the sympathetic nervous system can influence mechanisms that modulate the hematopoietic system to promote atherosclerosis and contribute to cardiovascular events.

**Abbreviations**

BM: bone marrow
CMP: common myeloid progenitor
CV: cardiovascular
CVD: cardiovascular disease
GMP: granulocyte-macrophage progenitor
MPC: myeloid progenitor cell
HSPC: hematopoietic stem and progenitor cell
WBC: white blood cell
SNS: sympathetic nervous system
G-CSF: granulocyte colony stimulating factor
TH: tyrosine hydroxylase
L-NAME: L-$N^G$-Nitroarginine methyl ester
Ach: acetylcholine
SNP: sodium nitroprusside
CRCs: concentration-response curves
BMEF: bone marrow extracellular fluid

## Introduction

Hypertension is a major, independent risk factor for atherosclerotic cardiovascular disease (CVD).[1] As the pathophysiology of hypertension is both complex and multifactorial, the direct mechanism(s) that ultimately contribute to CVD remain unclear.[2] The most frequently targeted pathway in reducing blood pressure is the renin-angiotensin system (RAS). The contribution of the RAS to hypertension and atherosclerosis is not exclusive, as angiotensin II (AngII) can also accelerate atherogenesis independent of hypertension.[3, 4] Another major determinant of hypertension is an overactive sympathetic nervous system (SNS).[5, 6] There are indications that autonomic input into the bone marrow (BM) may be altered in the setting of hypertension.[7-10] However, the mechanisms promoting atherogenesis with SNS activation associated hypertension are not completely elucidated. While there is an overlap in some atherosclerosis promoting mechanisms between the RAS and SNS, a distinct subset of events is also likely to be evoked by the SNS, which requires further investigation.

Atherosclerosis is a disease driven by the infiltration of immune cells, in particular monocytes into the plaque.[11-13] It is also well established that the abundance of circulating monocytes predicts cardiovascular (CV) events and is directly linked to atherogenesis.[14, 15] Interestingly, the SNS plays a direct role in regulating the hematopoietic system from which immune cells including monocytes arise.[16-19] In the context of CVD, the mobilization of hematopoietic stem and progenitor cells (HSPCs) from the BM to extramedullary tissues such as the spleen results in the generation of atherogenic monocytes that abundantly enter into the atherosclerotic plaque.[20] Mobilization of HSPCs can be mediated by sympathetic signaling within the BM, particularly in response to granulocyte-colony stimulating factor (G-CSF). The SNS synergizes with G-CSF to promote the breakdown of the HSPC BM microenvironment, which decreases the abundance of key HSPC retention factors and results in the liberation of HSPCs into the circulation.[16] This pathway has also been shown to be activated following a myocardial infarction (MI).[21] Sympathetic activation, along with raised G-CSF levels that are observed in apolipoprotein E knockout (*Apoe*$^{-/-}$) mice, caused HSPC mobilization from the BM and homing to the spleen, where monocytes were subsequently produced that infiltrated atherosclerotic lesions. Interestingly, this promoted an unstable plaque phenotype, prone to rupturing and thus, provides a plausible explanation for primary heart attack survivors being highly prone to a secondary, often fatal, CV event.[21, 22] Importantly, the involvement of the SNS in driving aberrant hematopoiesis is not restricted to complications following a MI, as similarities in other models of stress and ischemic stroke are evident, suggesting this to be a more general mechanism. The augmented hematopoietic response in these pathologies caused by overactivation of the SNS were inhibited by administration of β-blockers or genetic deletion of β-adrenergic receptors.[21, 23-25]

There appears to be an important role of the SNS in regulating hematopoiesis in acute stressors (i.e. MI, stroke, variable stress). However, it remains unknown if chronic sympathetic activation invokes this same atherogenic process. Thus, it is plausible that chronic sympathetic activation present in some cases of hypertension could play an important role in regulating atherogenesis by altering hematopoiesis. To address this question, we employed the Schlager hypertensive mice which were crossed onto an *Apoe*$^{-/-}$ background to produce hypertensive atherosclerosis-prone mice. The Schlager mouse was chosen as it represents a model of hypertension that is almost entirely driven by the SNS, with minimal contribution by the RAS.[26] We sought to characterize the contribution of SNS activation associated hypertension to the development of atherosclerosis, with the aim of

understanding whether this form of hypertension was also associated with alterations to the hematopoietic system. Moreover, we aimed to investigate whether targeting the SNS could inhibit atherogenesis, and in turn, reveal an additional mechanism of hypertension associated atherosclerosis.

## Methods

Detailed methods are available in *Online supplementary Methods*

**Animal Models:** *Apoe*$^{-/-}$ mice were purchased from Jackson Laboratories and bred at the AMREP Animal centre. To generate hypertensive *Apoe*$^{-/-}$ mice, BPH/2J mice were crossed with *Apoe*$^{-/-}$ mice to produce BPH/2J x *Apoe*$^{-/-}$ (BPH/*Apoe*$^{-/-}$) mice. At 6 weeks of age, male *Apoe*$^{-/-}$ and BPH/ *Apoe*$^{-/-}$ mice were placed on a western type diet (WTD - SF00-219, Specialty Feeds, Australia; 21% fat, 0.15% cholesterol) for 16 weeks. In the first cohort of mice, age-matched mice *Apoe*$^{-/-}$ and BPH/*Apoe*$^{-/-}$ were placed on a WTD for 16 weeks for end-point analysis. In a second cohort of mice, obtained from a new set of breeders, three groups of aged-matched mice were employed: 1) *Apoe*$^{-/-}$, 2) BPH/*Apoe*$^{-/-}$ and 3) BPH/ *Apoe*$^{-/-}$ + propranolol (0.5g/L; administered via drinking water for the duration of the WTD feeding). For the propranolol group, mice consumed on average 2.5ml of water amounting to an average daily dose of 35-40mg/kg/daily of propranolol.

To determine the effect of specific $\beta_2$-adrenoreceptor blockade on HSPC mobilization and blood pressure we used BPH mice on an *Apoe*$^{+/+}$ background. The mice were injected daily with ICI-118551 (5mg/kg; Abcam, AUS) for 2 weeks.

All animal experiments were approved by the AMREP Animal Ethics Committee and conducted in accordance with the Australian code of practice for the care and use of animals for scientific purposes as stipulated by the National Health and Medical Research Council of Australia. All mice were housed in a normal light and dark cycle and had ad libitum access to food and water. Mice were randomly assigned to treatment and end-point analysis was blinded.

**Statistics:** Data are presented as mean ± SEM (unless stated otherwise) and were analysed using the two-tailed Student t-test or One-way ANOVA where appropriate. Analysis of baseline and final blood pressure between strains was performed using a two-way ANOVA with the factors strain ($P_{strain}$) and time ($P_{time}$) followed by a Sidak post-hoc test to account for multiple comparisons. A $P<0.05$ was considered significant. All tests were performed using the Prism software (GraphPad Software, Inc., La Jolla, CA).

## Results

### Hypertension associated with chronic sympathetic activation promotes an unstable atherosclerotic phenotype

To determine the contribution of chronic sympathetic activation in hypertension to atherosclerosis we crossed Schlager hypertensive mice with *Apoe*$^{-/-}$ mice (BPH/*Apoe*$^{-/-}$) and

compared these to normotensive *Apoe*$^{-/-}$ mice. Mice were fed a high fat, high cholesterol western type diet (WTD) for 16 weeks. We preferenced this model over continual infusions of noradrenaline to allow for circadian fluctuations in blood pressure and heart rate, and to prevent the ongoing immune complications of surgery associated with the use of mini-pumps. Firstly, examining traditional cardiovascular risk factors revealed no change in body weight or cholesterol between the two groups and while blood pressure increased over the feeding period in both strains, the BPH/*Apoe*$^{-/-}$ mice maintained significantly higher blood pressure as measured by tail cuff and radio telemetry (**Figure 1, A-C** and Figure S1). The mice were also equally active (Figure S1). To explore the effect of chronic sympathetic activation associated with hypertension on atherosclerosis, we assessed the atherosclerotic burden in the proximal aorta and aortic arch. We observed increases in plaque size between the groups (**Figure 1D,E**), suggesting that sympathetically driven hypertension may promote accelerated plaque growth. We further explored the lesion characteristics and noted a significant increase in the abundance of lipid within the lesions from the BPH/*Apoe*$^{-/-}$ mice (**Figure 1F**). A significant increase in plaque macrophages were accompanied by a decrease in plaque collagen in the BPH/*Apoe*$^{-/-}$ mice (**Figure 1G,H**), suggesting that chronic sympathetic activation was promoting remodeling of lesions in an adverse, unstable manner. This plaque phenotype in the BPH/*Apoe*$^{-/-}$ mice resonates with the findings of Dutta *et al* in the context of acute SNS stimulation during a MI.[21]

**Hypertensive *Apoe*$^{-/-}$ mice do not develop endothelial dysfunction**

Endothelial dysfunction is a generally accepted consequence of hypertension.[27] To determine if the enhanced atherogenesis in BPH/*Apoe*$^{-/-}$ mice was the result of endothelial dysfunction we assessed the vascular responses in aortas from the BPH/*Apoe*$^{-/-}$ mice in comparison with control *Apoe*$^{-/-}$ mice. Firstly, no change in vessel diameter or constrictor responses to a high potassium solution was evident. Nor were there differences in basal nitric oxide (NO) levels when the constriction to L-NAME (L-N$^{G}$-Nitroarginine methyl ester) was examined (**Figure 2, A-C**). These data suggest that alterations in vascular reactivity are not biased by differences in constrictor responses. Surprisingly, endothelium-dependent NO-mediated relaxation in response to acetylcholine (ACh) was worse in the *Apoe*$^{-/-}$ mice when compared to BPH/*Apoe*$^{-/-}$ mice (**Figure 2D**). These differences between the strains were endothelium independent since there were no differences in the constriction and relaxation response to the NO donor sodium nitroprusside (SNP) in the presence or absence of L-NAME (**Figure 2E**). To further confirm no decline in vascular function in these mice, we examined the abundance of T cells, which have been linked to the pathogenesis of hypertension[28]. We observed no differences in aortic T cells between the *Apoe*$^{-/-}$ and BPH/*Apoe*$^{-/-}$ mice (**Figure 2F**). Moreover, there was no difference in the activation state of these CD4$^{+}$ T cells, as assessed by CD62L expression (MFI; *data not shown*). These data suggest that the enhanced atherogenesis in the BPH/*Apoe*$^{-/-}$ mice occurs independently of changes to the endothelium.

**BPH/*Apoe*$^{-/-}$ mice have enhanced myelopoiesis**

An overactive SNS has recently been shown to promote the mobilization of BM HSPCs to the spleen, resulting in the generation of splenic monocytes that can infiltrate into atherosclerotic lesions. Therefore, we next assessed the hematopoietic system in these mice.[21] We discovered prominent monocytosis and neutrophilia in the BPH/*Apoe*$^{-/-}$ mice in

the blood (**Figure 3A**). Next, to determine if the increased monocyte and neutrophil numbers were due to activated myelopoiesis, we examined the abundance and proliferation of HSPCs and myeloid progenitor cells in the BM. While the levels and proliferation of HSPCs within the BM were similar (**Figure 3B,C**), we did observe more granulocyte-macrophage progenitors (GMPs) in the BPH/*Apoe*$^{-/-}$ mice, which were proliferating at a higher rate (**Figure 3D,E**). Consistent with SNS activation in promoting the mobilisation of HSPCs from the BM, we detected elevated levels of circulating HSPCs and myeloid progenitors (MPCs) in the BPH/*Apoe*$^{-/-}$ mice (**Figure 3F**). Given the higher circulating HSPCs, we were expecting to see more HSPCs in the spleen. However, no such change in the abundance of HSPCs was detected (**Figure 3G**). Of note, a higher proportion were in the $G_2M$ phase of the cell cycle (**Figure 3H**), suggesting that the chronic activation of the SNS was influencing the HSPCs to proliferate more in the spleens of BPH/*Apoe*$^{-/-}$ mice. Indeed, monocytes and neutrophils were elevated in the spleens of the BPH/*Apoe*$^{-/-}$ mice, confirming extramedullary myelopoiesis was occurring in this chronic sympathetic driven model (**Figure 3I**).

**Sympathetic activation contributes to the breakdown of the HSPC bone marrow microenvironment**

The Schlager mice are an established model of sympathetic activation-mediated hypertension.[26] However, we wanted to confirm that there was evidence of increased sympathetic activation in the BM, which could account for the enhanced mobilization of HSPCs observed in Figure 3D. Firstly, to confirm an overall increase in sympathetic tone, we quantified plasma noradrenaline levels, which we found to be higher in the BPH/*Apoe*$^{-/-}$ mice (**Figure 4A**). More central to our proposed mechanism for enhanced HSPC mobilization in the BPH/*Apoe*$^{-/-}$ mice, we found enhanced expression of tyrosine hydroxylase (TH), the rate-limiting enzyme found in nerve terminals responsible for noradrenaline (NA) production, around the blood vessels in the BM of the BPH/*Apoe*$^{-/-}$ mice (**Figure 4B**). Together, these data reveal a more global increase in sympathetic tone in SNS-driven hypertension.

Next, we sought to determine if overactive sympathetic signalling in the BM led to changes within the BM microenvironment and whether these changes could be reversed with the use of a β-blocker. Given the importance of sympathetic overdrive in mediating hypertension, as expected, propranolol normalized blood pressure in the BPH/*Apoe*$^{-/-}$ mice (**Figure 4C**).

Having demonstrated that propranolol could reverse the systemic responsiveness of β-receptors to sympathetic activation in BPH/*Apoe*$^{-/-}$ mice, we examined key HSPC niche cells in the BM to determine if sympathetic overdrive influenced myelopoiesis via effects on the BM niche. Interestingly, we found a significant reduction in the abundance of $CD51^+$ osteoblasts in the BM on the BPH/*Apoe*$^{-/-}$ mice, which were restored when these mice were treated with propranolol (**Figure 4D**). Consistent with this finding, analysis of BM mRNA for *Runx2*, the transcription factor that drives osteoblast production, showed a reduction in *Runx2* expression in the BPH/*Apoe*$^{-/-}$ mice relative to *Apoe*$^{-/-}$ mice. Similar to our flow cytometry data, treatment with propranolol prevented the suppression of *Runx2* expression (**Figure 4E**). When we assessed the gross morphological changes in the BM, it appeared that the vascular structures were altered with the BPH/*Apoe*$^{-/-}$ mice showing smaller sinusoidal structures relative to the *Apoe*$^{-/-}$ mice, with propranolol reverting the sinusoids back to that seen in the *Apoe*$^{-/-}$ mice (**Figure 4F**). Furthermore, in examining the endothelial cell population, we noted a trend towards a decrease in the abundance of these cells, which,

again, could be restored with the administration of propranolol (**Figure 4G**). As these niche cells are an important source of the HSPC retention factor CXCL12, we measured its mRNA expression and found that propranolol greatly increased *Cxcl12* expression, thereby potentially aiding in promoting HSPC retention and reduced quiescence in the BM (Figure S2, A). The changes in these two key niche cells may provide a mechanism for increased HSPC release from the BM in BPH/*Apoe*$^{-/-}$ mice. Other cells within the BM express β-adrenoreceptors, which we profiled using gene array data from Novershtern *et al*. and analysed using online software (BloodSpot) to generate a hierarchical differentiation tree.[29, 30] Firstly, HSPCs and myeloid progenitors did not display any enrichment for the adrenoceptors. However, neutrophils were identified as one of the cells enriched in transcripts for the $\beta_2$-adrenoreceptor, but not $\beta_1$- or $\beta_3$-adrenoreceptors (Figure S2, B-D). We pharmacologically confirmed the requirement for $\beta_2$-adrenoreceptor stimulation in HSPC mobilization using the BPH mice on an *Apoe*$^{+/+}$ background by administering the $\beta_2$ specific antagonist ICI-118551 (Figure S2, E). Furthermore, neutrophils have previously been shown to be responsive to NA *in vitro*.[31, 32] Mechanistically, activated neutrophils can release MMP9 which can cleave CXCR4 on HSPCs, providing another avenue to HSPC liberation from the BM.[22, 33] We measured levels of MMP9 in the BM extracellular fluid (BMEF) via zymography and found that both active and latent MMP9 levels increased in the BPH/*Apoe*$^{-/-}$ mice, a phenotype reversed with propranolol treatment (**Figure 4H** and Figure S2, F). In support of this we found reduced surface CXCR4 expression on the HSPCs from the BPH/*Apoe*$^{-/-}$ mice, which was restored in mice treated with propranolol (**Figure 4I**). These data were further supported by BM mRNA analysis indicating that propranolol treatment increases *Cxcr4* expression (Figure S2G). To explore this mechanism further, we cultured HSPCs in the supernatants of neutrophils treated with NA and examined CXCR4 cell surface abundance. We found significantly less CXCR4 on HSPCs cultured in supernatants from NA activated neutrophils (isolated from wild-type mice), compared to vehicle treated neutrophils, which was prevented when MMP9 was inhibited (**Figure 4J**). When we included the $\beta_2$-adrenoreceptor specific inhibitor ICI-118551 into the BM neutrophil stimulation media with NA, the harvested supernatant caused less efficient cleavage of CXCR4 (Figure S2H) thereby confirming the role for neutrophil $\beta_2$-adrenoreceptors. These data support the hypothesis that, sympathetic activation is present in the BM of the BPH/*Apoe*$^{-/-}$ mice and responsible for the mobilization of HSPCs by acting on key niche cells along with stimulating neutrophils to secrete proteases that cleave the retention receptor CXCR4 on HSPCs.

**Suppressing chronic sympathetic signaling dampens myelopoiesis in hypertensive *Apoe*$^{-/-}$ mice**

Having observed a restoration in the HSPC BM microenvironment when BPH/*Apoe*$^{-/-}$ mice were treated with propranolol, we explored if this was also reflected by normalization of myelopoiesis in these mice. Following treatment with propranolol we observed a reduction in circulating monocytes and neutrophils (**Figure 5A**). We determined if this reduction was echoed by changes in the BM stem and progenitor populations. Following administration of propranolol the abundance of BM HSPCs was not affected, however these cells were proliferating at lower rates and giving rise to fewer GMPs (**Figure 5, B-D**). Consistent with an improvement in the HSPC microenvironment, there were fewer mobilized HSPCs and MPCs in the blood of the BPH/*Apoe*$^{-/-}$ mice treated with propranolol (**Figure 5E**). This was paralleled by a decrease in extramedullary hematopoiesis in the spleen as evidenced by fewer proliferating HSPCs, GMPs and less monocytes and neutrophils (**Figure 5, F-I**).

Taken together, these data suggest that lowering responsiveness to chronic sympathetic signaling in the BPH/*Apoe*$^{-/-}$ mice results in an overall dampening of myelopoiesis.

**Blocking sympathetic signalling decreases atherosclerosis in BPH/*Apoe*$^{-/-}$ mice**

To examine if the reduction in sympathetic tone and dampening of myelopoiesis was associated with reduced atherosclerotic plaque progression, we assessed the size and complexity of lesions in the proximal aorta. Firstly, we noted a reduction in lesion size in the proximal aorta and aortic arch of BPH/*Apoe*$^{-/-}$ mice treated with propranolol (**Figure 6A, B**). Exploring the lesion characteristics, we noted that propranolol treated mice had reduced plaque lipid accumulation along with a reduction in plaque macrophages (**Figure 6C, D**). We also observed a trend for increased collagen (**Figure 6E**). These changes were seen in the absence of any changes in plasma cholesterol levels (**Figure 6F**). Given that the hypertension in the BPH/*Apoe*$^{-/-}$ mice did not promote endothelial dysfunction, it suggests that the improvements in plaque size and complexity are due to dampened myelopoiesis and subsequently, reduced monocyte infiltration.

## Discussion

Chronic hypertension is arguably one of the most common risk factors associated with atherosclerotic CVD.[1] However, delving into the responsible mechanism(s), it remains unclear if an increase in blood pressure alone, or in conjunction with a change in concurrent signalling events such activation of the RAS or sympathetic activation, directly contributes to atherosclerotic CVD. Using a genetic model of hypertension driven by sympathetic activation, we show that this form of hypertension (compared to atherosclerotic prone mice without hypertension) alters the characteristics of the atherosclerotic lesion to a more unstable phenotype, hallmarked by increased macrophage accumulation. We also found that chronic sympathetic activation caused changes in hematopoiesis. In particular, increased sympathetic activity was found in the BM, altering the HSPC microenvironment and causing the liberation of certain stem cells to the spleen where monocytes were generated. This was accompanied by an increase in blood monocytes, likely explaining the increased macrophage burden observed in the atherosclerotic lesions. These atherogenic pathways could all be inhibited pharmacologically by blocking sympathetic signalling through β-adrenoreceptors using propranolol. These findings suggest that chronic sympathetic activation, present in many forms of hypertension, likely contributes to the increased CVD risk by modulating hematopoiesis, independent of endothelial dysfunction.

With respect to understanding the contribution of hypertension to vascular disease, the majority of research has focused on the effects on the endothelium. Perhaps the most common belief is that hypertension causes endothelial dysfunction and activation, which in turn recruits immune cells and forms the main mechanism propagating the atheroma. Interestingly, we found no evidence of endothelial dysfunction in our hypertensive mice, at least in this model of a dominant sympathetic driven form of hypertension the endothelial dysfunction was not contributing significantly to atherogenisis.[34] Supporting our theory that underlying sympathetic nervous signalling, that may be independent of pressure itself, can drive atherogenesis, moderate increases in AngII are sufficient to promote accelerated atherogenesis, without elevations in blood pressure.[3, 4] Additionally, AngII has also been shown to invoke a T- helper cell ($T_H1$) immune response to promote atherogenesis independent of its hemodynamic effects. Thus signalling events that can cause hypertension

are likely important in driving CVD through their immune modulatory responses.[7-10, 35, 36] Further, with the discovery of accelerated vascular disease driven by acute events triggering sympathetic activation leading to enhanced monocyte production, it is plausible that this pathway is triggered in chronic SNS-driven hypertension and would contribute to accelerated atherosclerosis.[21, 23, 24] We hypothesized that the overactive SNS seen in subgroups of patients with hypertension would contribute to atherogenesis by stimulating hematopoiesis. Importantly, elevated WBCs are associated with the incidence of hypertension and predicts CV outcomes in this patient group.[37-39] However, the cause of increased WBCs in hypertensive patients has not been resolved.

Consistent with recent studies which have observed monocytosis following acute scenarios of sympathetic activation, we too observed monocytosis in the hypertensive BPH/*Apoe*$^{-/-}$ mice.[21, 24] The initial predominant change driven by the overactive sympathetic signalling in our study, relevant to increased myelopoiesis, appears to occur within the BM. We noted a decreased abundance of two key niche cells, endothelial cells and osteoblasts, which harbour anchoring points in the marrow for HSPCs, preventing their release into circulation.[40-43] The contribution of the SNS in regulating this process was first described by a seminal study from the Frenette laboratory, detailing the requirement of a functional SNS in the BM, which is required for G-CSF mediated HSPC mobilization.[16] Almost a decade later the Nahrendorf group discovered the importance of this pathway in respect to CVD, revealing that sympathetic activation following an acute myocardial infarction promotes HSPC liberation to the spleen where the production of an additional atherogenic pool of monocytes occurs.[21] The absence of an expanded HSPC population in the spleen is likely due to the chronic nature of our study and suggests that these cells likely rapidly matured into myeloid committed progenitors. The recent studies then suggest that the monocytes generated, migrate into the atherosclerotic lesion, and enhanced macrophage burden, potentiating the risk of a secondary CV event. Our data reveal that this process is occurring chronically and identifies an important mechanism that likely contributes to atherogenesis and the increased risk of a CV event in hypertension. We also identified another pathway by which sympathetic signalling can induce the liberation of BM HSPCS by causing a decrease in the HSPC-expressed retention receptor CXCR4. Given that HSPCs do not appear to express β adrenoreceptors, it suggested a cell extrinsic mechanism resulting in less HSPC cell surface CXCR4. Interestingly, neutrophils express $\beta_2$ adrenoceptors and can be activated after sensing NE (Figure S2, B-C). Modelling this *in vitro* revealed that NE-activated neutrophils produce MMP9, which cleaves CXCR4 on HSPCs. Thus, BM sympathetic activation likely liberates HSPCs via multiple mechanisms, some of which are independent of the previously described SNS/G-CSF axis.

As mentioned above, there are several studies that have identified a role for β adrenoreceptors in influencing HSPC release via modulating the BM niche. There is strong evidence for the role of β-3 adrenergic receptor in regulating nestin$^{+}$ stromal cell production of key factors such as CXCL12, angiopoietin and stem cell factor, thereby influencing HSPC retention and proliferation. β-3 antagonism following ischemic events has shown reduced HSPC mobilisation and proliferation leading to dampened extramedullary hematopoiesis.[19, 21, 23, 24] However, there is also strong evidence pointing to a role for the β-2 adrenergic receptor in regulating BM niche components and HSPC mobilisation. Although this has been suggested to occur through other niche components such as osteoblasts and other stromal cells and not specifically nestin$^{+}$ cells.[16, 18] These findings regarding the role of β

adrenoceptors in modulating HSPC mobilisation suggest that in our study there is a likely contribution of both β-2 and β-3 receptors to changes in the BM. However, considering the role of β-2 in the setting of hypertension and elevated blood pressure we focused on the specific role of β-2. Interestingly, a recent study by Mendez-Ferrer's group has also highlighted the chronic role of nestin$^{+}$ cells present in the BM and other tissues in regulating myeloid cell movement in the setting of atherosclerosis.[44] Given that nestin$^{+}$ cells in the BM express β-3 receptors and the data we have presented above regarding chronic sympathetic driven hypertension and its contribution to atherosclerosis, it is likely that this pathway may also play a role and warrants further investigation.

The obvious limitation of this study is that our findings were generated in mice. However, this also allowed us to isolate a prominent form of hypertension to reveal a novel atherogenic mechanism, which appears to be independent of endothelial dysfunction, and thus our findings also permit the current dogma to be challenged. While we revealed the effectiveness of propranolol in this model, there is a need to further investigate the effects of directly reducing enhanced hematopoiesis without targeting systemic blood pressure. It is likely that with the development of anti-inflammatory drugs targeted at the hematopoietic system, it would be possible to dampen the effects on the hematopoietic system without affecting blood pressure which would hypothetically provide the same conclusions as in the present study. Finally, we only studied one form of hypertension, driven by sympathetic signaling. It would be of specific importance to extend a modified version of this hypothesis to hypertension driven by the RAS.

## Acknowledgements

A) Sources of funding: A.J.M is Career Development Fellow of the NHMRC (APP1085752) and a Future Leader Fellowship from the National Heart Foundation (100440) and a recipient of a CSL Centenary Award. This study was also supported by NHMRC project grants (APP1106154 and APP1142938) to A.J.M. and J.C-D. M.J.K is a Russell Berrie Foundation Scholar in Diabetes Research from the Naomi Berrie Diabetes Centre. PRN was supported by grants from the NIH (R01HL1379 & R00HL1225).
B) Disclosures: None

## References


1. (2015) WHO. Non Communicable diseases in Health in 2015: From MDG to SDG. Contract No: ISBN 978954156511. 2015;
2. Bondjers G, Glukhova M, Hansson GK, Postnov YV, Reidy MA, Schwartz SM. Hypertension and atherosclerosis. Cause and effect, or two effects with one unknown cause? Circulation. 1991;84(6 Suppl):VI2-16.
3. Daugherty A, Manning MW, Cassis LA. Angiotensin II promotes atherosclerotic lesions and aneurysms in apolipoprotein E-deficient mice. J Clin Invest. 2000;105(11):1605-1612.
4. Mazzolai L, Duchosal MA, Korber M, et al. Endogenous angiotensin II induces atherosclerotic plaque vulnerability and elicits a Th1 response in ApoE-/- mice. Hypertension. 2004;44(3):277-282.
5. Noll G, Wenzel RR, Binggeli C, Corti C, Luscher TF. Role of sympathetic nervous system in hypertension and effects of cardiovascular drugs. Eur Heart J. 1998;19 Suppl F:F32-38.
6. Esler M, Jennings G, Korner P, et al. Assessment of human sympathetic nervous system activity from measurements of norepinephrine turnover. Hypertension. 1988;11(1):3-20.
7. Zubcevic J, Jun JY, Kim S, et al. Altered inflammatory response is associated with an impaired autonomic input to the bone marrow in the spontaneously hypertensive rat. Hypertension. 2014;63(3):542-550.
8. Santisteban MM, Zubcevic J, Baekey DM, Raizada MK. Dysfunctional brain-bone marrow communication: a paradigm shift in the pathophysiology of hypertension. Curr Hypertens Rep. 2013;15(4):377-389.
9. Santisteban MM, Kim S, Pepine CJ, Raizada MK. Brain-Gut-Bone Marrow Axis: Implications for Hypertension and Related Therapeutics. Circ Res. 2016;118(8):1327-1336.
10. Santisteban MM, Ahmari N, Carvajal JM, et al. Involvement of bone marrow cells and neuroinflammation in hypertension. Circ Res. 2015;117(2):178-191.
11. Ross R. Atherosclerosis is an inflammatory disease. Am Heart J. 1999;138(5 Pt 2):S419-420.
12. Woollard KJ, Geissmann F. Monocytes in atherosclerosis: subsets and functions. Nat Rev Cardiol. 2010;7(2):77-86.
13. Murphy AJ, Tall AR. Disordered haematopoiesis and athero-thrombosis. Eur Heart J. 2016;37(14):1113-1121.
14. Qiao JH, Tripathi J, Mishra NK, et al. Role of macrophage colony-stimulating factor in atherosclerosis: studies of osteopetrotic mice. Am J Pathol. 1997;150(5):1687-1699.
15. van der Valk FM, Kuijk C, Verweij SL, et al. Increased haematopoietic activity in patients with atherosclerosis. Eur Heart J. 2017;38(6):425-432.
16. Katayama Y, Battista M, Kao WM, et al. Signals from the sympathetic nervous system regulate hematopoietic stem cell egress from bone marrow. Cell. 2006;124(2):407-421.
17. Stiekema LCA, Schnitzler JG, Nahrendorf M, Stroes ESG. The maturation of a 'neural-hematopoietic' inflammatory axis in cardiovascular disease. Curr Opin Lipidol. 2017;28(6):507-512.
18. Mendez-Ferrer S, Battista M, Frenette PS. Cooperation of beta(2)- and beta(3)-adrenergic receptors in hematopoietic progenitor cell mobilization. Ann N Y Acad Sci. 2010;1192:139-144.
19. Mendez-Ferrer S, Lucas D, Battista M, Frenette PS. Haematopoietic stem cell release is regulated by circadian oscillations. Nature. 2008;452(7186):442-447.
20. Robbins CS, Chudnovskiy A, Rauch PJ, et al. Extramedullary hematopoiesis generates Ly-6C(high) monocytes that infiltrate atherosclerotic lesions. Circulation. 2012;125(2):364-374.

21. Dutta P, Courties G, Wei Y, et al. Myocardial infarction accelerates atherosclerosis. Nature. 2012;487(7407):325-329.
22. Westerterp M, Gourion-Arsiquaud S, Murphy AJ, et al. Regulation of hematopoietic stem and progenitor cell mobilization by cholesterol efflux pathways. Cell Stem Cell. 2012;11(2):195-206.
23. Heidt T, Sager HB, Courties G, et al. Chronic variable stress activates hematopoietic stem cells. Nat Med. 2014;20(7):754-758.
24. Courties G, Herisson F, Sager HB, et al. Ischemic stroke activates hematopoietic bone marrow stem cells. Circ Res. 2015;116(3):407-417.
25. Esler M, Jennings G, Lambert G. Measurement of overall and cardiac norepinephrine release into plasma during cognitive challenge. Psychoneuroendocrinology. 1989;14(6):477-481.
26. Davern PJ, Nguyen-Huu TP, La Greca L, Abdelkader A, Head GA. Role of the sympathetic nervous system in Schlager genetically hypertensive mice. Hypertension. 2009;54(4):852-859.
27. Brandes RP. Endothelial dysfunction and hypertension. Hypertension. 2014;64(5):924-928.
28. Guzik TJ, Hoch NE, Brown KA, et al. Role of the T cell in the genesis of angiotensin II induced hypertension and vascular dysfunction. J Exp Med. 2007;204(10):2449-2460.
29. Novershtern N, Subramanian A, Lawton LN, et al. Densely interconnected transcriptional circuits control cell states in human hematopoiesis. Cell. 2011;144(2):296-309.
30. Bagger FO, Sasivarevic D, Sohi SH, et al. BloodSpot: a database of gene expression profiles and transcriptional programs for healthy and malignant haematopoiesis. Nucleic Acids Res. 2016;44(D1):D917-924.
31. Kim MH, Gorouhi F, Ramirez S, et al. Catecholamine stress alters neutrophil trafficking and impairs wound healing by beta2-adrenergic receptor-mediated upregulation of IL-6. J Invest Dermatol. 2014;134(3):809-817.
32. Nicholls AJ, Wen SW, Hall P, and MJH, Wong CHY. Activation of the sympathetic nervous system modulates 1 neutrophil function. J Leukoc Biol. 2018;103(2):295-309.
33. Levesque JP, Hendy J, Takamatsu Y, Simmons PJ, Bendall LJ. Disruption of the CXCR4/CXCL12 chemotactic interaction during hematopoietic stem cell mobilization induced by GCSF or cyclophosphamide. J Clin Invest. 2003;111(2):187-196.
34. Susic D. Hypertension, aging, and atherosclerosis. The endothelial interface. Med Clin North Am. 1997;81(5):1231-1240.
35. Zubcevic J, Santisteban MM, Pitts T, et al. Functional neural-bone marrow pathways: implications in hypertension and cardiovascular disease. Hypertension. 2014;63(6):e129-139.
36. Wei Z, Spizzo I, Diep H, Drummond GR, Widdop RE, Vinh A. Differential phenotypes of tissue-infiltrating T cells during angiotensin II-induced hypertension in mice. PloS One. 2014;9(12):e114895.
37. Schillaci G, Pirro M, Pucci G, et al. Prognostic value of elevated white blood cell count in hypertension. Am J Hypertens. 2007;20(4):364-369.
38. Karthikeyan VJ, Lip GY. White blood cell count and hypertension. J Hum Hypertens. 2006;20(5):310-312.
39. Nakanishi N, Sato M, Shirai K, Suzuki K, Tatara K. White blood cell count as a risk factor for hypertension; a study of Japanese male office workers. J Hypertens. 2002;20(5):851-857.
40. Calvi LM, Adams GB, Weibrecht KW, et al. Osteoblastic cells regulate the haematopoietic stem cell niche. Nature. 2003;425(6960):841-846.
41. Semerad CL, Christopher MJ, Liu F, et al. G-CSF potently inhibits osteoblast activity and CXCL12 mRNA expression in the bone marrow. Blood. 2005;106(9):3020-3027.
42. Hooper AT, Butler JM, Nolan DJ, et al. Engraftment and reconstitution of hematopoiesis is dependent on VEGFR2-mediated regeneration of sinusoidal endothelial cells. Cell Stem Cell. 2009;4(3):263-274.

43. Tamplin OJ, Durand EM, Carr LA, et al. Hematopoietic stem cell arrival triggers dynamic remodeling of the perivascular niche. Cell. 2015;160(1-2):241-252.
44. Del Toro R, Chevre R, Rodriguez C, et al. Nestin(+) cells direct inflammatory cell migration in atherosclerosis. Nat Commun. 2016;7:12706.

## Figure legends:

**Figure 1. Hypertensive *Apoe*$^{-/-}$ mice have characteristics of unstable atherosclerotic lesions.** *Apoe*$^{-/-}$ and *BPH/Apoe*$^{-/-}$ mice were fed a WTD for 16wks **A)** Weekly body mass progression. **B)** Total plasma cholesterol was measured at the end of feeding. **C)** Systolic blood pressure of mice were measured before and at the end of WTD feeding. **D)** H&E staining for plaque size in the proximal aorta and **E)** ORO$^{+}$ lesions in the aortic arch were quantified. Proximal aortas were also stained for **F)** lipid content (ORO), **G)** macrophages (CD68) and **H)** collagen (picosirius red). Lesions were imaged at X4 (insets) and zoomed in to view single lesions, scale bar = 100μm. Data are presented as mean ± SEM where *p<0.05 and **p<0.01 (Student's t-test) ****p<0.0001 (Two-way ANOVA). A,B,C) n= 5-10, D,E,F) n= 8, G) n=9, H) n=7-8.

**Figure 2. Hypertensive *Apoe*$^{-/-}$ do not have endothelial dysfunction.** *Apoe*$^{-/-}$ and *BPH/Apoe*$^{-/-}$ mice were fed a WTD for 16wks after which aortas were harvested for *ex vivo* assessment of endothelial function. Aortas were assessed for **A)** diameter, **B)** KPSS and **C)** L-NAME contraction. Further myograph analyses were preformed to determine aortic relaxation in response to **D)** ACh and **E)** SNP with or without L-NAME administration. Aortic T cell infiltration was assessed by flow cytometry for **F)** Abundance of CD4$^{+}$ T-helper cells. Data are presented as mean ± SEM where **p<0.01 (Student's t-test). A,B) n=6-10,C) n= 6-8, D) n= 4-6, E,F) n=6.

**Figure 3. *BPH/Apoe*$^{-/-}$ mice have extramedullary hematopoiesis.** *Apoe*$^{-/-}$ and *BPH/Apoe*$^{-/-}$ mice were fed a WTD for 16wks after which flow cytometry was used to assess **A)** circulating monocytes(M)/neutrophils(N). **B)** Levels of BM HSPCs and **C)** proportion of HSPCs proliferating. **D)** Levels of BM GMPs and **E)** proportion of GMPs proliferating. **F)** Blood HSPC and MPC populations. **G)** Spleen HSPCs and GMPs were assessed along with **H)** proliferating HSPCs and GMPs. **I)** splenic monocyte(M)/neutrophil(N) populations. Data are presented as mean ± SEM where *p<0.05 and **p<0.01 (Student's t-test). A-I) n= 5-11.

**Figure 4. Sympathetic nervous system signalling induces a breakdown of the HSPC niche in the BM.** *Apoe*$^{-/-}$ and *BPH/Apoe*$^{-/-}$ mice were fed a WTD for 16wks with *BPH/Apoe*$^{-/-}$ mice either treated with or without Propranolol (0.5g/L) in drinking water. **A)** Plasma NA was quantified by HPLC. **B)** BM sections were immunostained for sympathetic activity as indicated by tyrosine hydroxylase, imaged at X20; scale bar = 25μm. **C)** Systolic blood pressure of mice following 16wks treatment. **D)** Osteoblastic lineage cells were quantified by flow cytometry. **E)** mRNA levels of *Runx2* in the BM. **F)** H&E stained representation of BM vascular morphology, imaged at X10 scale bar = 100μm. **G)** BMECs were measured by flow cytometry. **H)** MMP9 content in the BM extracellular fluid was determined via Zymography. **I)** CXCR4 expression levels on HSPCs was assessed by flow cytometry from and **J)** neutrophil supernatant cultured HSPCs. Data are presented as mean ± SEM where *p<0.05, **p<0.01, ***p<0.001, ****p<0.0001 (Student's t-test or One-Way ANOVA). A) n= 8, B) n=5, C) n=7, D) n= 7-9, E) n= 5-9, G) n= 7-9, H) 5-9, I) n= 12-15, J) n= 7.

**Figure 5. Propranolol prevents extramedullary hematopoiesis in *BPH/Apoe*$^{-/-}$ mice.** *BPH/Apoe*$^{-/-}$ mice were fed a WTD for 16 wks and treated with vehicle or Propranolol (0.5g/L) in drinking water. Flow cytometry was used to assess **A)** circulating monocytes(M)/neutrophils(N), **B)** BM HSPCs and **C)** proportion of which are proliferating along with **D)** of BM GMPs. **E)** Blood HSPC and MPC populations. **F)** Spleen HSPC and **G)** GMP populations along with **H)** proliferating splenic HSPCs and GMPs were assessed by flow cytometry. **I)** Splenic monocyte(M)/neutrophil(N) populations. Data are presented as mean ± SEM where *p<0.05, **p<0.01 and ***p<0.001 (Student's t-test). A-I) n= 6-10.

**Figure 6. Propranolol inhibits plaque progression in *BPH/Apoe*$^{-/-}$ mice.** *BPH/Apoe*$^{-/-}$ mice were fed a WTD for 16 wks and treated with vehicle or Propranolol (0.5g/L) in drinking water. At the end point, atherosclerosis in the proximal aorta was assessed for **A)** H&E staining for plaque size in the proximal aorta and **B)** lipid content (ORO$^{+}$) lesions in the aortic arch were quantified. Proximal aortas were also stained for **C)** lipid content (ORO), **D)** macrophages (CD68) and **E)** collagen (picosirius red). Lesions were imaged at X4 (insets) and zoomed in to view single lesion, scale bar = 100μm. **F)** Total plasma cholesterol levels. Data are presented as mean ± SEM where *p<0.05 and **p<0.01 (Student's t-test). A,B) n= 9, C-E) n=7, F) n=9.

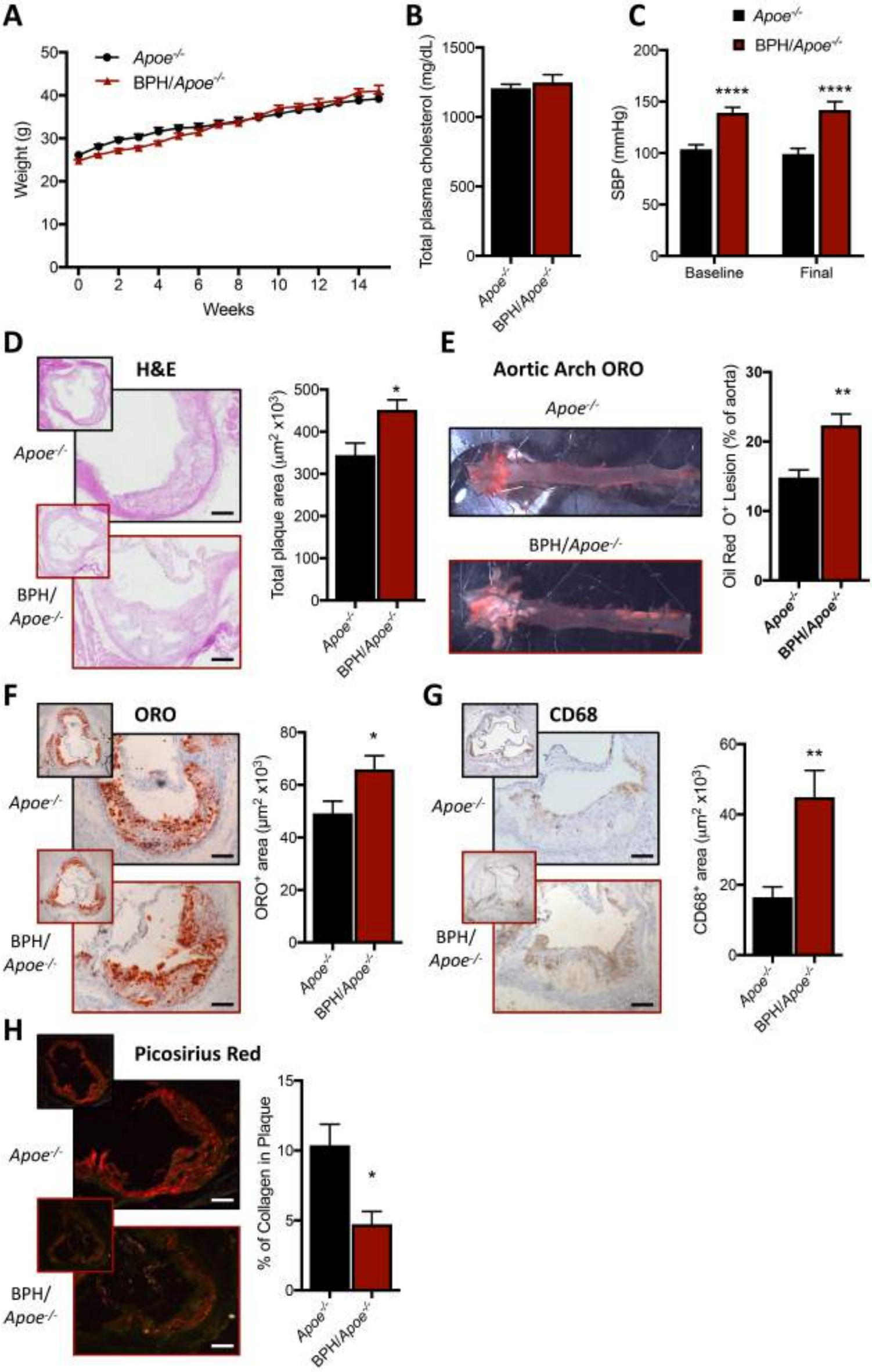
A
Apoe-/-
BPH/Apoe-/-
Weight (g)
Weeks
B
Total plasma cholesterol (mg/dL)
C
SBP (mmHg)
****
Baseline
Final
D
H&E
Apoe-/-
BPH/Apoe-/-
Total plaque area (μm2 x103)
*
E
Aortic Arch ORO
Oil Red O+ Lesion (% of aorta)
**
F
ORO
ORO+ area (μm2 x103)
G
CD68
CD68+ area (μm2 x103)
H
Picosirius Red
% of Collagen in Plaque

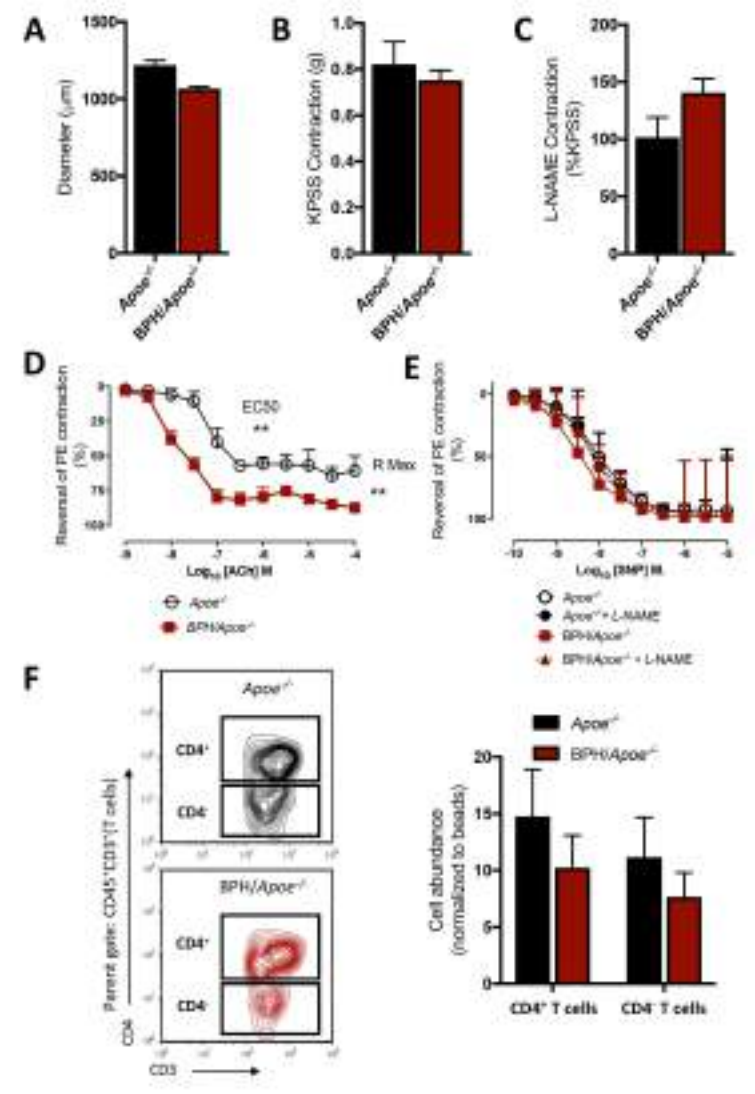
A
Diameter (μm)
1500
1000
500
0
Apoe-/-
BPH/Apoe-/-
B
KPSS Contraction (g)
1.0
0.8
0.6
0.4
0.2
0.0
Apoe-/-
BPH/Apoe-/-
C
L-NAME Contraction (%KPSS)
200
150
100
50
0
Apoe-/-
BPH/Apoe-/-
D
Reversal of PE contraction (%)
EC50
**
R Max
**
Log10 [ACh] M
Apoe-/-
BPH/Apoe-/-
E
Reversal of PE contraction (%)
Log10 [BMP] M
Apoe-/-
Apoe-/- + L-NAME
BPH/Apoe-/-
BPH/Apoe-/- + L-NAME
F
Apoe-/-
CD4+
CD4-
BPH/Apoe-/-
CD4+
CD4-
Parent gate: CD45+CD3+(T cells)
CD4
CD3
Apoe-/-
BPH/Apoe-/-
Cell abundance (normalized to beads)
20
15
10
5
0
CD4+ T cells
CD4- T cells

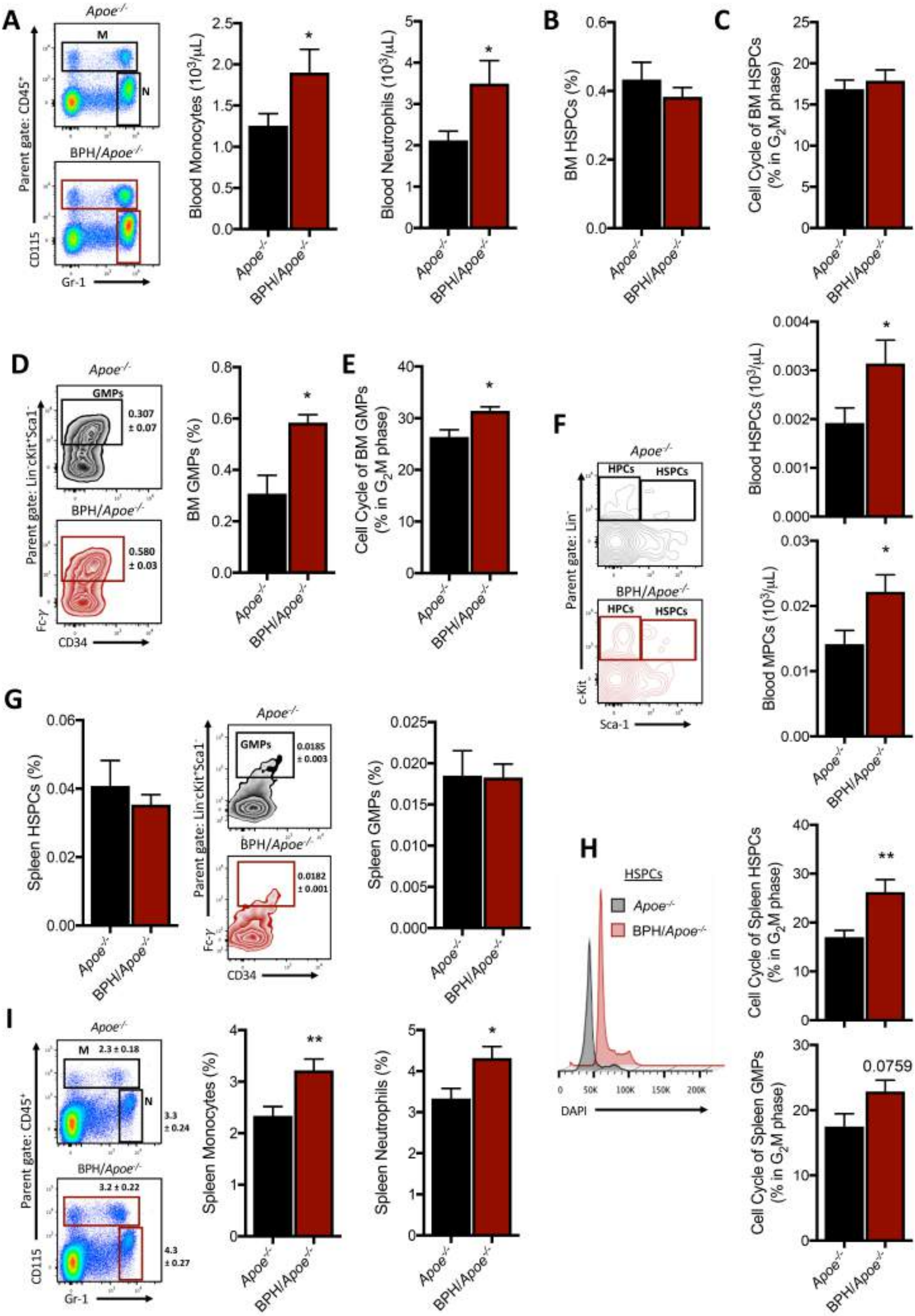
A
Apoe-/-
M
N
Parent gate: CD45+
BPH/Apoe-/-
CD115
Gr-1
Blood Monocytes (10^3/μL)
Blood Neutrophils (10^3/μL)
B
BM HSPCs (%)
C
Cell Cycle of BM HSPCs (% in G2M phase)
D
GMPs
0.307 ± 0.07
0.580 ± 0.03
Parent gate: Lin-cKit+Sca1-
Fc-γ
CD34
BM GMPs (%)
E
Cell Cycle of BM GMPs (% in G2M phase)
F
HPCs
HSPCs
Parent gate: Lin-
c-Kit
Sca-1
Blood HSPCs (10^3/μL)
Blood MPCs (10^3/μL)
G
Spleen HSPCs (%)
0.0185 ± 0.003
0.0182 ± 0.001
Spleen GMPs (%)
H
HSPCs
DAPI
Cell Cycle of Spleen HSPCs (% in G2M phase)
I
2.3 ± 0.18
3.3 ± 0.24
3.2 ± 0.22
4.3 ± 0.27
Spleen Monocytes (%)
Spleen Neutrophils (%)
Cell Cycle of Spleen GMPs (% in G2M phase)
0.0759

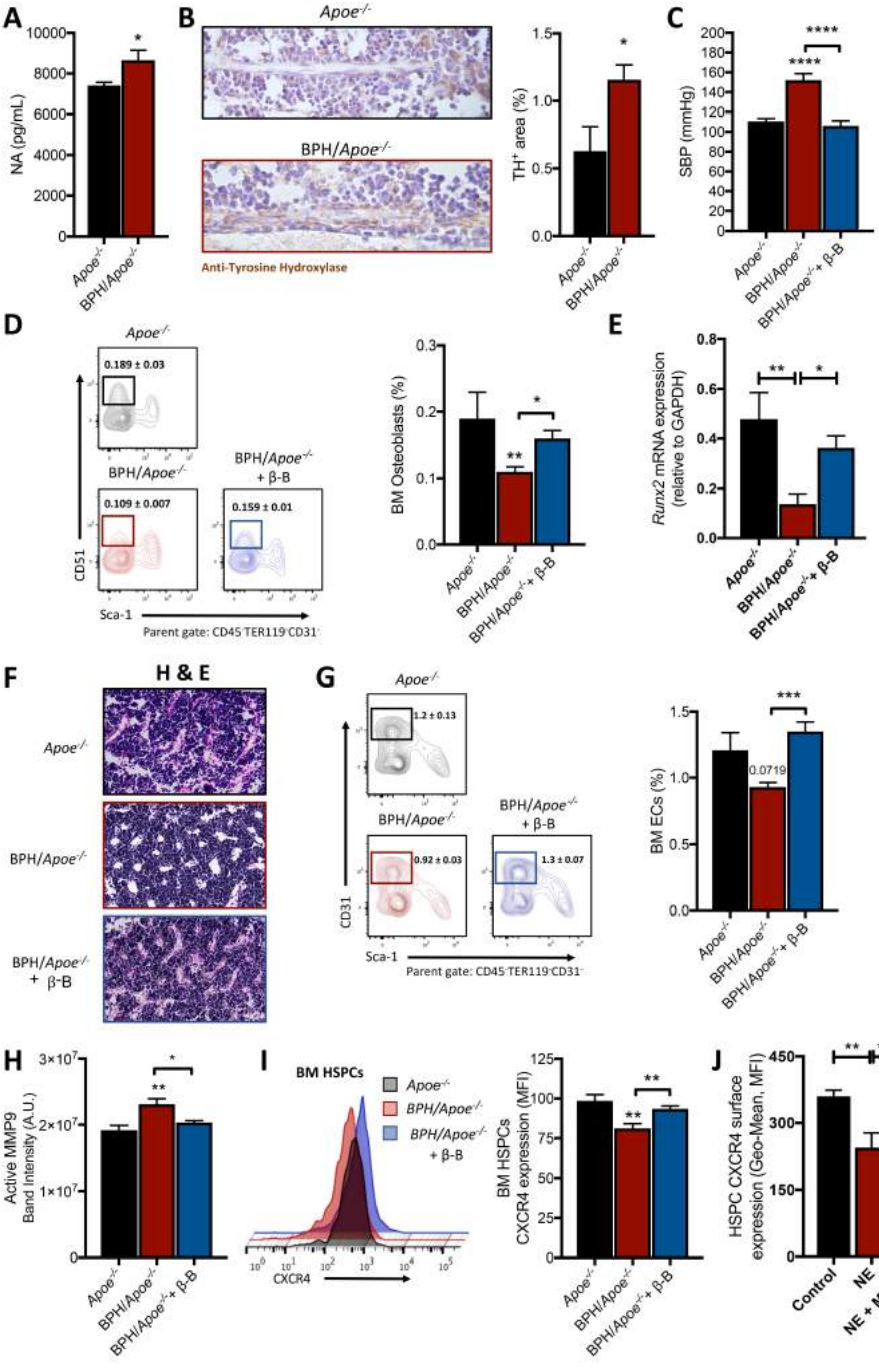
A
NA (pg/mL)
10000
8000
6000
4000
2000
0
*
Apoe-/-
BPH/Apoe-/-
B
Apoe-/-
BPH/Apoe-/-
Anti-Tyrosine Hydroxylase
TH+ area (%)
1.5
1.0
0.5
0.0
*
C
SBP (mmHg)
200
180
160
140
120
100
80
60
40
20
0
****
****
Apoe-/-
BPH/Apoe-/-
BPH/Apoe-/- + β-B
D
Apoe-/-
0.189 ± 0.03
BPH/Apoe-/-
0.109 ± 0.007
BPH/Apoe-/- + β-B
0.159 ± 0.01
CD51
Sca-1
Parent gate: CD45-TER119-CD31-
BM Osteoblasts (%)
0.3
0.2
0.1
0.0
**
*
E
Runx2 mRNA expression (relative to GAPDH)
0.8
0.6
0.4
0.2
0.0
**
*
F
H & E
Apoe-/-
BPH/Apoe-/-
BPH/Apoe-/- + β-B
G
Apoe-/-
1.2 ± 0.13
BPH/Apoe-/-
0.92 ± 0.03
BPH/Apoe-/- + β-B
1.3 ± 0.07
CD31
Sca-1
Parent gate: CD45-TER119-CD31-
BM ECs (%)
1.5
1.0
0.5
0.0
0.0719
***
H
Active MMP9 Band Intensity (A.U.)
3×10^7
2×10^7
1×10^7
0
**
*
I
BM HSPCs
Apoe-/-
BPH/Apoe-/-
BPH/Apoe-/- + β-B
CXCR4
BM HSPCs CXCR4 expression (MFI)
125
100
75
50
25
0
**
**
J
HSPC CXCR4 surface expression (Geo-Mean, MFI)
450
300
150
0
**
****
Control
NE
NE + MMP9i

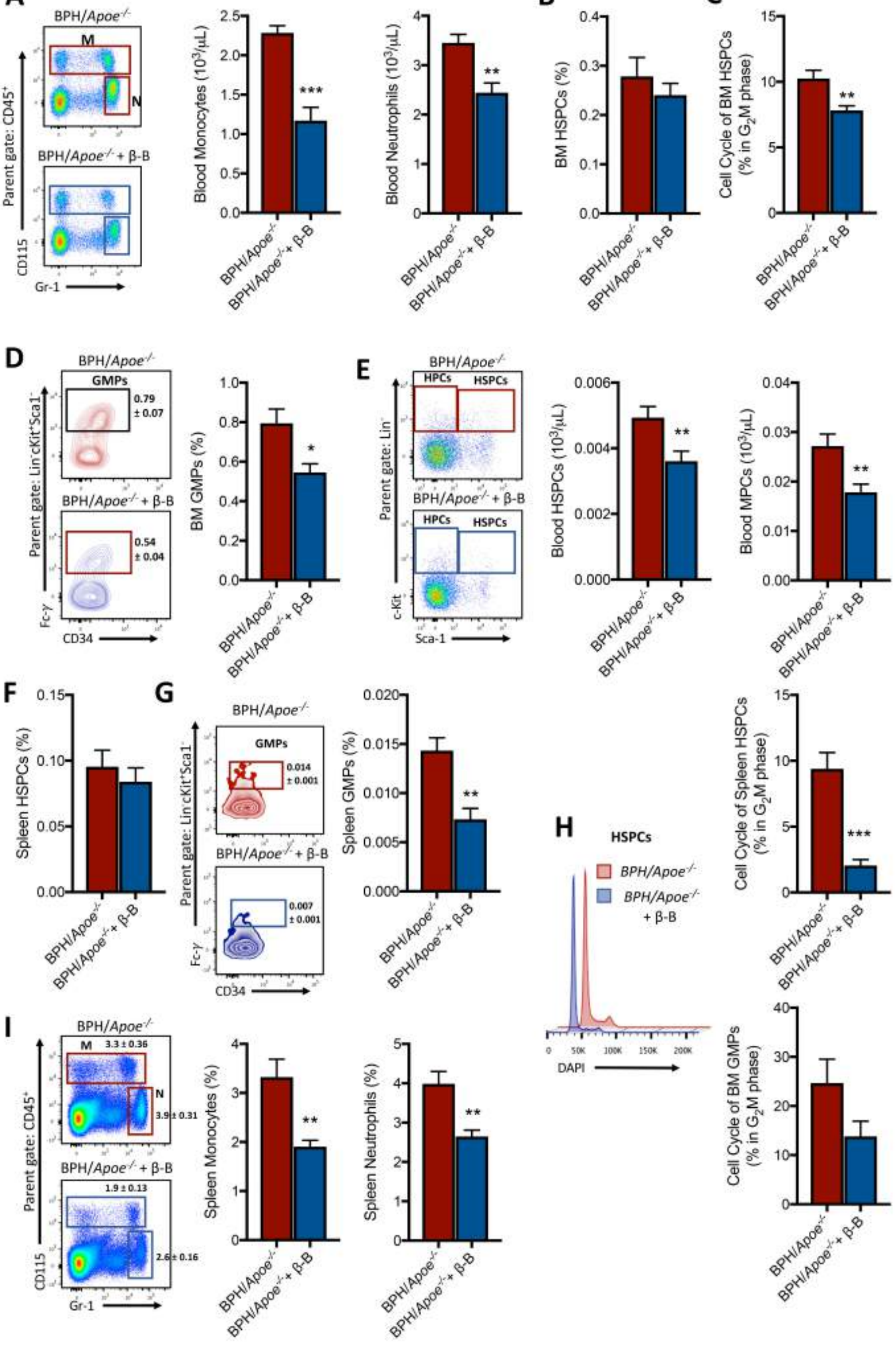
A
BPH/Apoe-/-
M
N
Parent gate: CD45+
CD115
Gr-1
BPH/Apoe-/- + β-B
Blood Monocytes (10³/μL)
***
BPH/Apoe-/-
BPH/Apoe-/- + β-B
Blood Neutrophils (10³/μL)
**
B
BM HSPCs (%)
C
Cell Cycle of BM HSPCs (% in G2M phase)
D
BPH/Apoe-/-
GMPs
0.79 ± 0.07
Parent gate: Lin-cKit+Sca1-
Fc-γ
CD34
BPH/Apoe-/- + β-B
0.54 ± 0.04
BM GMPs (%)
*
E
BPH/Apoe-/-
HPCs
HSPCs
Parent gate: Lin-
c-Kit
Sca-1
BPH/Apoe-/- + β-B
Blood HSPCs (10³/μL)
Blood MPCs (10³/μL)
F
Spleen HSPCs (%)
G
BPH/Apoe-/-
GMPs
0.014 ± 0.001
Parent gate: Lin-cKit+Sca1-
Fc-γ
CD34
BPH/Apoe-/- + β-B
0.007 ± 0.001
Spleen GMPs (%)
H
HSPCs
BPH/Apoe-/-
BPH/Apoe-/- + β-B
DAPI
Cell Cycle of Spleen HSPCs (% in G2M phase)
***
I
BPH/Apoe-/-
M
3.3 ± 0.36
N
3.9 ± 0.31
Parent gate: CD45+
CD115
Gr-1
BPH/Apoe-/- + β-B
1.9 ± 0.13
2.6 ± 0.16
Spleen Monocytes (%)
Spleen Neutrophils (%)
Cell Cycle of BM GMPs (% in G2M phase)

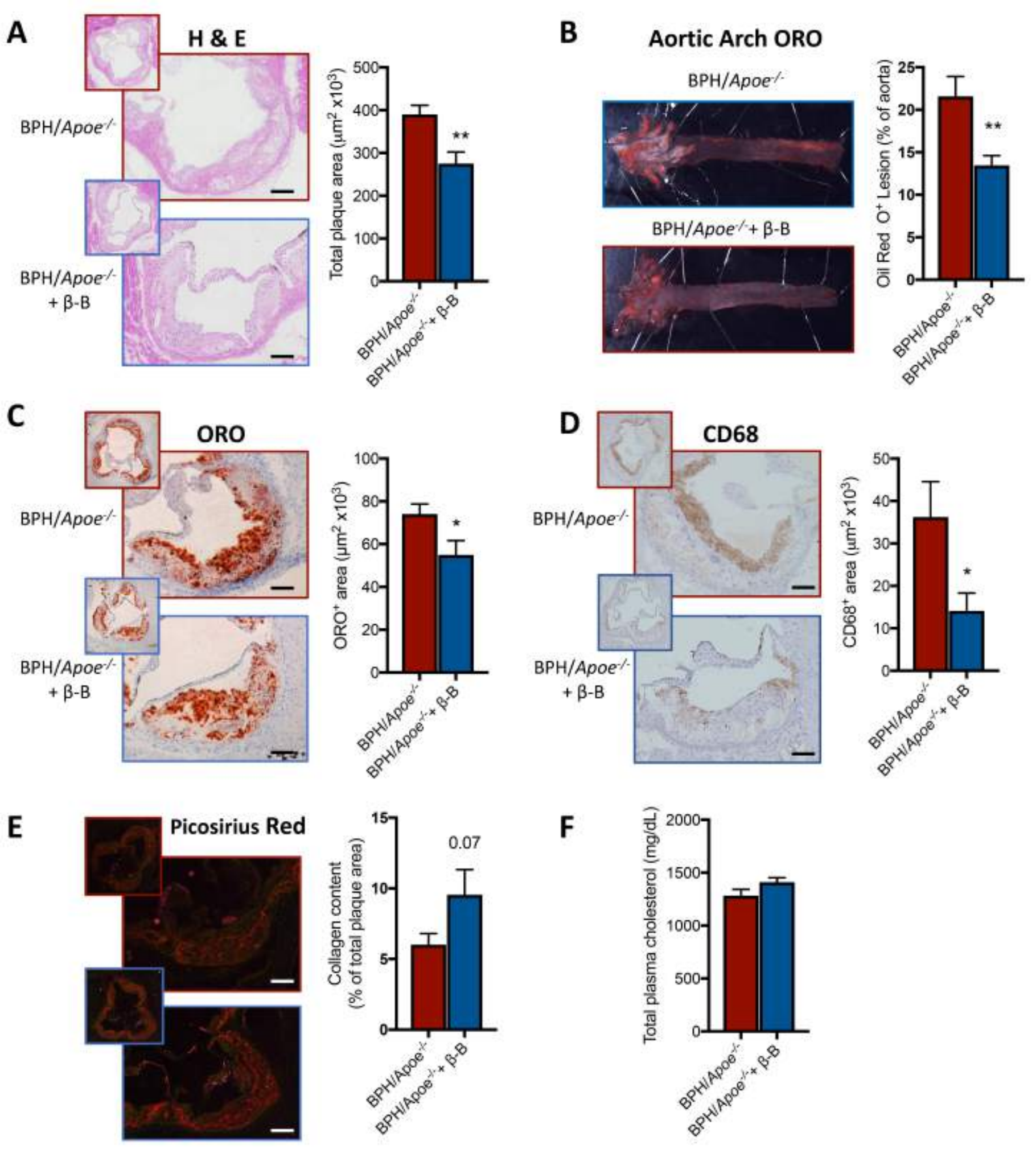
A
H & E
BPH/Apoe-/-
BPH/Apoe-/- + β-B
Total plaque area (μm2 x103)
500
400
300
200
100
0
**
BPH/Apoe-/-
BPH/Apoe-/- + β-B
B
Aortic Arch ORO
BPH/Apoe-/-
BPH/Apoe-/- + β-B
Oil Red O+ Lesion (% of aorta)
25
20
15
10
5
0
**
BPH/Apoe-/-
BPH/Apoe-/- + β-B
C
ORO
BPH/Apoe-/-
BPH/Apoe-/- + β-B
ORO+ area (μm2 x103)
100
80
60
40
20
0
*
BPH/Apoe-/-
BPH/Apoe-/- + β-B
D
CD68
BPH/Apoe-/-
BPH/Apoe-/- + β-B
CD68+ area (μm2 x103)
50
40
30
20
10
0
*
BPH/Apoe-/-
BPH/Apoe-/- + β-B
E
Picosirius Red
Collagen content (% of total plaque area)
15
10
5
0
0.07
BPH/Apoe-/-
BPH/Apoe-/- + β-B
F
Total plasma cholesterol (mg/dL)
2000
1500
1000
500
0
BPH/Apoe-/-
BPH/Apoe-/- + β-B

**Supplementary file**

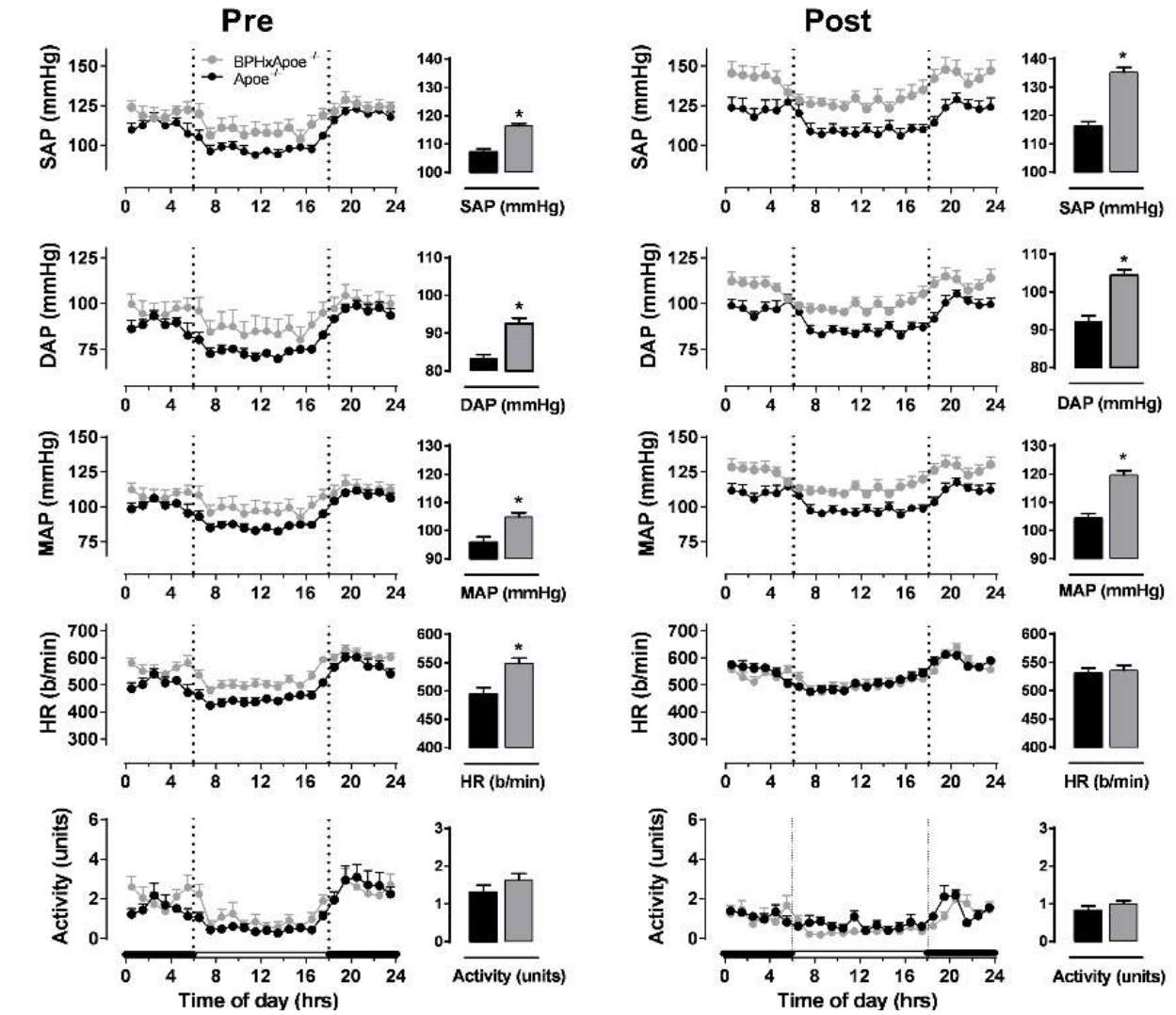


**Figure S1. Cardiovascular characteristics.** *Apoe*$^{-/-}$ and *BPH/Apoe*$^{-/-}$ mice were fed a WTD for 16 wks. Using radiotelemetry mice were assessed for SAP, DAP, MAP along with HR and activity. These measurements were recorded pre and post-WTD. Data are presented as mean ± SEM where *$p<0.05$ (Student's t-test) n=10

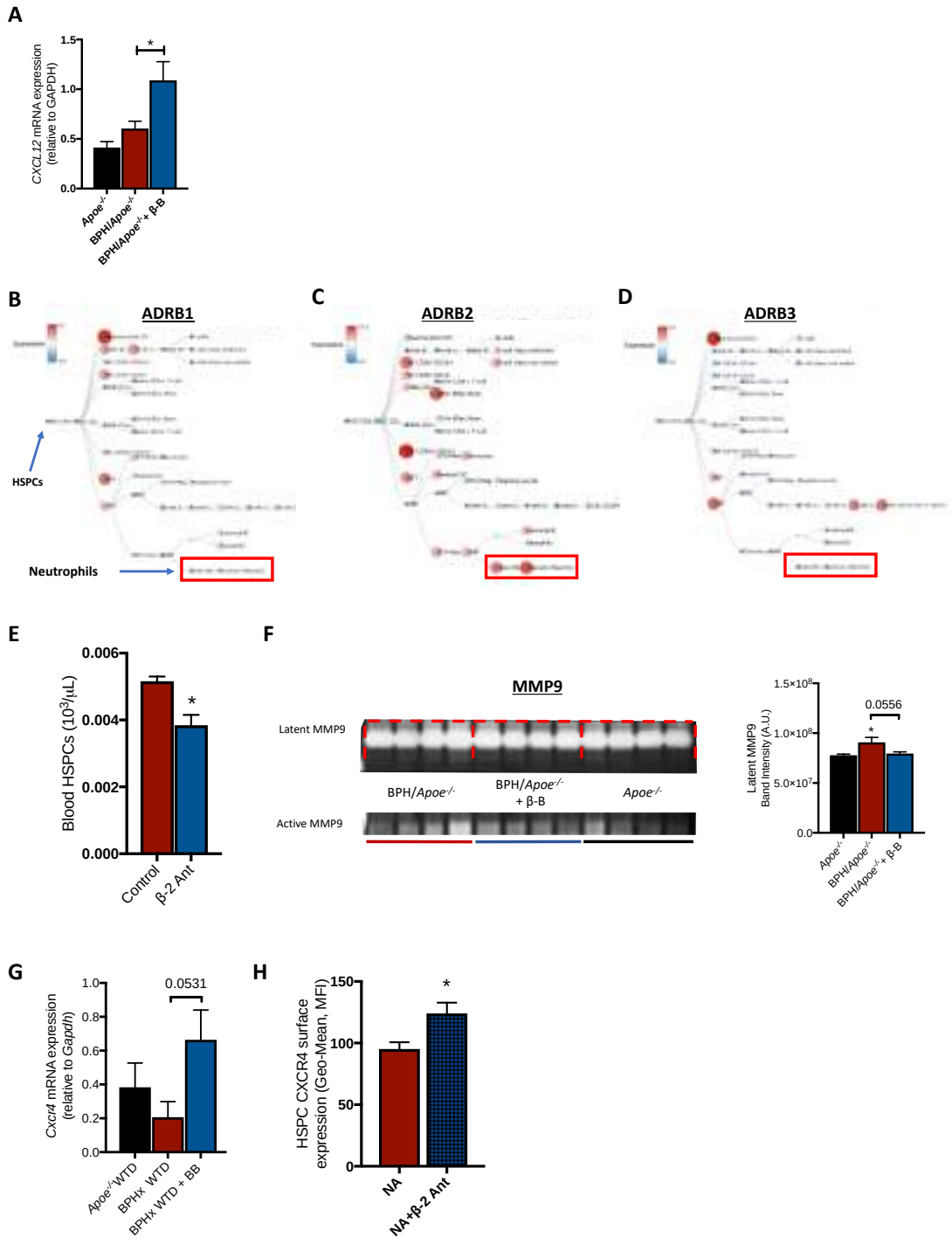


**Figure S2. Bone marrow microenvironment alteration in sympathetic activation. A)** Real time qPCR was used to assess mRNA expression levels of BM *Cxcl12*. **B-D)** BloodSpot (Online software) generation of a hierarchal myeloid tree depicting the expression of the adrenergic receptors β-1, β-2, β-3. **E)** *BPH/Apoe*$^{+/+}$ mice were treated with the $\beta_2$ specific antagonist ICI-118551 for 2 weeks and blood HSPCs assessed via flow cytometry. **F)** Latent MMP9 levels assessed by gelatin zymography. **G)** mRNA expression levels of BM *Cxcr4*. **H)** BM neutrophils were stimulated with NA ± ICI-118551 and the harvested supernatant was incubated with BM HSPCs to assess CXCR4 cleavage via flow cytometry**.** Data are presented as mean ± SEM where *p<0.05 measured by a One-Way ANOVA. **A)** n=5-9**, E)** n=4, **F)** n= 4, **G)** n=5-9, **H)** n=6.

| Antibodies | Cat # | Clone | Source | Fluorochrome |
|---|---|---|---|---|
| CD45 | 103126 | 30-F11 | BioLegend | PB |
| Gr1 | 552093 | RB6-8C5 | BD Pharmingen | PerCP-Cy5.5 |
| CD115 | 12-1152-82 | AFS98 | eBioscience | PE |
| Gr1 | 553127 | RB6-8C5 | BD Bioscience | FITC |
| CD2 | 11-0021-85 | RM2-5 | eBioscience | FITC |
| CD3 | 11-0033-82 | eBio500A2 | eBioscience | FITC |
| CD19 | 101506 | MP19-1 | BioLegend | FITC |
| TER119 | 11-5921-85 | TER-119 | eBioscience | FITC |
| CD45R | 11-0452-85 | RA3-6B2 | eBioscience | FITC |
| CD8a | 553030 | 53-6.7 | BD Bioscience | FITC |
| CD4 | 11-0042-85 | RM4-5 | eBioscience | FITC/PE-Cy7 |
| Sca1 | 108120 | D7 | BioLegend | PB |
| ckit | 105826 | 2B8 | BioLegend | APC/CY7 |
| Fcγ | 560540 | 2.4G2 | BD Biosciences | Percp-Cy5.5 |
| CD31 | 46-0311-82 | 390 | eBioscience | Percp-Cy5.5 |
| CD51 | 12-0512-83 | RMV-7 | eBioscience | PE |
| F4/80 | 123114 | BM8 | BioLegend | PE-Cy7 |
| CXCR4 | 12-9991-82 | 2B11 | eBioscience | PE |

**Table S1. Antibody details**

| Gene | Primer Sequence – forward | Primer sequence – Reverse |
|---|---|---|
| GAPDH | 5’ – TGA AGC AGG CAT CTG AGG G | 5’ – CGA AGG TGG AAG AGT GGG AG |
| CXCL12 | 5’ – CGC CAA GGT CGT CGC CG | 5’ – TTG GCT CTG GCG ATG TGG C |
| CXCR4 | 5’ – CAC GGC TGT AGA GCG AGT GT | 5’ – TGC CGA CTA TGC CAG TCA AG |
| Runx2 | 5’ – TCC GAA ATG CCT CCG CTG TTA T | 5’ – GGA CCG TCC ACT GTC ACT TTA A |

**Table S2. qRT-PCR primer sequences**

## Methods

**Animal Models:** *Apoe*$^{-/-}$ mice were purchased from Jackson Laboratories and bred at the AMREP Animal centre. To generate hypertensive *Apoe*$^{-/-}$ mice, BPH/2J mice were crossed with *Apoe*$^{-/-}$ mice to produce BPH/2J x *Apoe*$^{-/-}$ (BPH/*Apoe*$^{-/-}$) mice. At 6 weeks of age, male *Apoe*$^{-/-}$ and BPH/ *Apoe*$^{-/-}$ mice were placed on a western type diet (WTD - SF00-219, Specialty Feeds, Australia. 21% fat, 0.15% cholesterol) for 16 weeks. In the first cohort of mice, age-matched mice *Apoe*$^{-/-}$ and BPH/*Apoe*$^{-/-}$ were placed on a WTD for 16 weeks for end-point analysis. In a second cohort of mice, obtained from a new set of breeders, three groups of aged-matched mice were employed: 1) *Apoe*$^{-/-}$, 2) BPH/*Apoe*$^{-/-}$and 3) BPH/ *Apoe*$^{-/-}$ + propranolol (0.5g/L; administered via drinking water for the duration of the WTD feeding). For the propranolol group, mice consumed on average 2.5ml of water amounting to an average daily dose of 35-40mg/kg/daily of propranolol.

To determine the effect of specific $\beta_2$-adrenoreceptor blockade on HSPC mobilization and blood pressure we used BPH mice on an *Apoe*$^{+/+}$ background. The mice were injected daily with ICI-118551 (5mg/kg; Abcam, AUS) for 2 weeks.

All animal experiments were approved by the AMREP Animal Ethics Committee and conducted in accordance with the Australian code of practice for the care and use of animals for scientific purposes as stipulated by the National Health and Medical Research Council of Australia. All mice were housed in a normal light and dark cycle and had ad libitum access to food and water.

**Lesion Analysis:** Mice were perfused with saline before heart and aorta collection. The aorta was dissociated from the heart at the point of entry between the highest point of the atria and fixed in PFA for further analysis (described below). The heart was dissected so that the upper region of the heart containing the aortic sinus was retained and frozen in optimal cutting temperature (OCT) compound. Serial 6µm sections of the proximal aorta were harvested on a cryostat at -20°C. Images were captured on an Olympus BX61 microscope, whereas collagen was imaged using polarised light. Image quantification was performed using Adobe Photoshop CC.

**H&E staining:** Sections were fixed (4min, 10% neutral buffered formalin), washed in PBS (4min), stained in Mayer's Haematoxylin (15min) and washed with running tap water before blueing in Scott's tap water for 30secs. The slides were then put in 95% ethanol (10 dips), stained in buffered alcoholic eosin (8min), dehydrated in absolute ethanol, cleared with xylene and coverslips were mounted using depex.

**Oil Red O (lipid) staining:** Sectioned lesions were fixed in 10% buffered formalin (4mins), washed in PBS (4min), dipped in 60% isopropanol before staining in 60% ORO working solution (2hrs, stock solution: 1% ORO powder in isopropanol). The slides were then washed in 60% isopropanol and distilled water. Sections were stained in Mayer's Haematoxylin (4mins), washed in tap and distilled water (3min each) and mounted with aquamount.

**CD68 (macrophage) staining:** Sections were thawed and fixed with paraformaldehyde (4%, 20min), washed in PBS (2x5min), incubated in pre-chilled 3% $H_2O_2$ in methanol (20min) and then washed in PBS (2x5min). Each section was blocked with normal goat serum (NGS, 10%,

30min), incubated with AVIDIN blocking solution (15min), rinsed in PBS and then incubated with rat anti-mouse CD68 primary antibody (1:200, 5% NGS, 4°C) overnight. The slides were then washed in PBS (2x5min) before being incubated with the secondary antibody (1:100, 5% NGS, 30min). Next, the sections were washed in PBS (2x5min), incubated with ABC avidin/biotin complex (30min) and DAB solution. Staining reaction was terminated with distilled water. The sections were counterstained with Mayer Haematoxylin for 15sec and rinsed in tap water before blueing in scotts tap water and washing in tap water. Finally, slides were dehydrated in ethanol (95% 3min, 100% 3x3min), cleared in xylene (2x5min) and mounted with depex.

**Picosirius (collagen) staining:** Sections were thawed and fixed in pre-chilled acetone (15min), washed in PBS (2x5min), stained in 0.1% Sirius red F3BA (1hr) and then washed in 0.01M HCl (2min). Subsequently, the slides were then dehydrated in alcohol (95%, 5mins; 100%, 2x5min), cleared in xylene (2x5min) and mounted with depex. Sections were imaged on Olympus BX61 microscope under brightfield and polarised light.

**Aortic Arch Lipid Analysis:** Lipid content, as a readout of atherosclerotic plaques in the aortic arch was measured by *en face* analysis. Dissected aortas were fixed in PFA, with fat and connective tissue removed from the outer layers of the vessel prior to staining. The aorta was then cut longitudinally and stained with ORO. After washing, the stained aortas were mounting on a silicone coated dish. Aortas were viewed on an Olympus SZX10 and captured using Q-Capture Pro 7 (QImaging) software. Quantification of ORO staining was performed off-line using Adobe Photoshop CC5.

**Total Plasma Cholesterol:** The Wako total cholesterol kit was used to measure plasma cholesterol as previously described[26].

**Blood Pressure Measurements:**
*Tail Cuff method:* Systolic blood pressure (SBP) was measured in all mice (prior to WTD administration) and after 16 weeks of feeding using the non-invasive tail cuff plethysmography technique. A MC4000 blood pressure analysis system (Hatteras Instruments) was used with a 37°C pre-heated stage. Mice were placed in restrainers with tails placed through a cuff and onto a heart rate monitor. Mice remained in restraints for 5 mins to allow acclimatisation after which 5 preliminary BP measurement cycles were run to ensure BP was detectable. Ten measurement cycles were then performed to ensure correct readings, the average of the readings for systolic, diastolic and mean arterial blood pressure were recorded.

*Blood pressure telemetry:* Under isoflurane open circuit anaesthesia (1.5-2.5%) *Apoe*$^{-/-}$ and BPH/*Apoe*$^{-/-}$ mice were implanted with radiotelemetry devices weighing 1.4g and approximately 10mm in length (TA11PA-C10; DataSciences International (DSI), St Paul, USA) as previously described.[27] Following a 10-day recovery from surgery, 1 min averages of pulsatile arterial blood pressure readings and locomotor activity were recorded continuously over a 72-hour period sampled at 100 Hz as previously described.[28] Mean arterial pressure and heart rate were analysed in Labview.[29]

**Vessel reactivity:**
*Preparation of vessels:* Mice were ethuanased via $CO_2$ asphyxiation which was confirmed by cessation of corneal and pedal reflexes. The thoracic aorta was removed and placed in ice-

cold Krebs solution (composition in mM: NaCl 119, KCl 4.7, $KH_2PO_4$ 1.18, $MgSO_4$ 1.17, $NaHCO_3$ 25, $CaCl_2$ 2.5, EDTA 0.026 and glucose 5.5). Perivascular fat and adhering connective tissue were removed from the aorta and it was cut into rings 2 mm in length. Each ring was mounted onto two parallel stainless-steel wires (200 µm in diameter) in a 5 ml chamber of a 4 channel myograph (Mulvaney Myograph, model 610M, JP trading), containing oxygenated Krebs solution and maintained at 37°C. Changes in tension were recorded using a PowerLab 8/35 (ADI Instruments Inc) connected to a computer.

*Myograph:* Tissues were equilibrated at resting tension for 30mins before undergoing a "normalisation" procedure to determine optimal resting tension and vessel diameter. During the normalisation procedure, tissues are subjected to a series of stretches beginning at wire touch and progressing to tensions of 30mN. Once tissues were set at their optimal resting tension, they were equilibrated for a further 30 min before their viability was tested with a high potassium physiological salt solution, (KPSS, composition in mM: KCl 123, $MgSO_4$ 1.17, $KH_2PO_4$ 2.37, $CaCl_2$ 2.5, EDTA 0.02 and glucose 5.5). Once the contractile response had plateaued, the chamber was rinsed three times with normal Krebs solution and the tissue was allowed to return to baseline. For relaxation curves, tissues were pre-constricted to 50% of the KPSS contraction using PE. Once the contraction had plateaued, cumulative concentration-response curves were acquired to ACh (1nM-10µM) or SNP (0.1nM-10µM) in the presence or absence of L-NAME. Only one protocol was completed in each aortic ring to avoid tolerance.

**White Blood Cell Counts:** White blood cell (WBC) counts were obtained from blood collected via cardiac puncture immediately following euthanasia. The counts were quantified on a Sysmex XS-1000*i* automated hematology analyser (Japan).

**Flow Cytometry:** All samples were run and analyzed on a BD FACS Canto II flow cytometer or Fortessa X-20 as stated below. Flow cytometry antibodies were all used at 1:400 dilutions and details of antibodies are available in Supplementary table 1.

*T-Cell Populations:* Aortas were harvested from the mice following cardiac puncture and flushing with saline. Aortas were digested in Liberase (Sigma-Aldrich, USA, Cat # 5401160001) for 45 mins at 37°C after which the cells were spun down, washed and resuspended in FACS Buffer (1x HBSS + 0.5mM EDTA and 0.05% BSA). Viable cells were gated using a live/dead stain (Ghost violet 510 viability dye, Tonbo Biosciences) on the Canto II where $CD4^-$ T cells were gated as $CD45^+CD3^+$ $CD4^-$ and $CD4^+$ T cells as $CD45^+CD3^+$ $CD4^+$.

*Monocyte Populations:* Bone marrow and spleen cells were obtained by mashing whole spleen through a 40µm strainer and then lysed using 1x RBC lysis buffer. Blood was collected via cardiac puncture into EDTA-lined tubes and placed directly on ice to prevent leukocyte activation and loss of cell surface CD115. The samples remained on ice or at 4°C for the remainder of the procedure. Red blood cells (RBCs) were lysed, and the washed cells were then stained with CD45, CD115 and Gr1 (Ly6-C/G) for 30 min on ice. The cells were washed, resuspended in FACS buffer and run on a Canto II flow cytometer (Figure 3) or a Fortessa X-20 (Figure 5). Leukocyte populations were identified as previously described.[20, 26, 30] Briefly, viable, single cells were selected on the basis of forward and side scatter characteristics, from which $CD45^+$ leukocytes were selected. Monocytes were identified as being $CD115^+$ with Ly6-

$C^{hi}$ monocytes identified as $Gr1^+$ and Ly6-$C^{lo}$ monocytes identified as $Gr1^-$. Neutrophils were identified as $CD115^-Gr1^+$.

*Hematopoietic stem and progenitor cells Populations:* Organs were collected and processed as mentioned above. Samples were then stained with a cocktail of antibodies (30 mins on ice) before analysis by flow cytometry as previously described[20, 26, 30]. Briefly, lineage committed cells were identified as (CD45R, CD19, CD11b, CD3e, TER-119, CD2, CD8, CD4 and Ly6-C/G, all FITC positive) with antibodies against Sca1 and cKit to identify myeloid progenitor cells ($Lineage^-$, $Sca1^-$, $cKit^+$) and HSPCs ($Lineage^-$, $Sca1^+$, $cKit^+$). GMPs were identified as ($Lineage^-$, $Sca1^-$, $cKit^+$, $Fc\gamma^{hi}$).

Proliferating stem and progenitor cells were assessed by intracellular DAPI (1:1000) staining performed following fixation and permeablization using a BD Fix/Perm kit (BD Biosciences, USA, Cat #. 554722). Samples were run on the Canto II (Figure 3) or Fortessa X-20 (Figure 5).

*Bone marrow niche cells:* A cocktail of antibodies were used to stain for osteoblast and endothelial cells containing lineage committed cells (CD45R, CD11b, CD3e, TER-119, CD8, CD4, CD45 and Ly-6G; all FITC; eBioscience), as well as Sca1-PB, CD51-PE, F4/80-PE/Cy7 and CD31-PerCP (Biolegend). Osteoblasts were identified as $Lin^-Sca1^-F4/80^-CD31^-CD51^+$. Endothelial cells were identified as $Lin^-Sca1^-F4/80^-CD31^+CD51^-$. Samples were run on the Fortessa X-20.

**Bone Analysis**

*Processing:* Femurs were harvested, fixed in 2% PFA overnight, and immersed in 0.5M EDTA in PBS with 1% PFA for 14 days for decalcification prior to paraffin embedding. The paraffin-embedded sections (5µm thickness) were deparaffinized, rehydrated, and stained.

*Bone H&E staining:* Sections were in Mayer's hematoxylin for 8 mins followed by a 2 min incubation in scott's tap water. Slides were then stained in eosin for 6 mins, dehydrated, cleared in xylene and mounted with DPX.

*Bone Tyrosine Hydroxylase staining:* Sections were deparaffinised in histolene and dehydrated using an ethanol gradient. Antigen retrieval was performed by immersing sections in 10mM EDTA at 90°C for 9 minutes in a pressure vessel. Slides were allowed to cool to room temperature. Sections were incubated in 3% $H_2O_2$ in methanol to quench endogenous peroxidases. Next, the sections were incubated in 10% normal goat serum for one hour followed by Tyrosine hydroxylase (rabbit anti-mouse) primary antibody (1:100, Millipore; AB9983) incubation overnight at 4°C. Following this, sections were incubated with biotinylated goat anti-Rabbit Secondary antibody (1:200; BA-1000 Vector Labs) for 1 hour at room temperature. Sections were then treated with an Avidin-biotin complex (Vectastain ABC HRP kit; PK-4000; Vector Labs) for 30mins followed by DAB treatment (SK-4100; Vector Labs) for 5mins. After washing samples were mounted with DPX mounting media.

**Neutrophil derived MMP9 effect on HSPC CXCR4:**

*Isolation of bone marrow neutrophils:* Neutrophils were isolated from the BM of C57BL/6 wildtype mice using the Ficoll method. Cells were overlaid on 3 mL of Ficoll-Paque Plus solution (GE Healthcare), and centrifuged for 20 min with no brakes at 600 g, at room temperature. Cell pellets were washed with PBS and RBC lysed for 1 min. Cells were then re-suspended in media for use. Further details can be found in the supplementary information.

*Noradrenaline activation of neutrophils:* The catecholamine was prepared by the dissolution of crystalline noradrenaline (NA; Sigma) in PBS. Neutrophils were stimulated with 10 μM of NA for 24 h. To assess the contribution of the $\beta_2$-adrenoreceptor to neutrophil responses to NA, we pre-treated (30 mins) the neutrophil suspension with ICI-118551 (100μM) and then co-incubated with NA and ICI-118551 for 24 h (10μM and 100μM respectively).

*Treatment of HSPCs with activated neutrophil supernatant:* BM suspension from flushed bones (described above) were incubated in the supernatant of neutrophils treated with 0 or 10 μM of NA for 45 mins at 37°C. To test the activity of MMP9, supernatant from NA treated neutrophils was pre-incubated with an MMP inhibitor (50μM; ab142180; Abcam, AUS) for 45 mins prior to incubation with BM suspension. BM was incubated for a further 45 mins in the presence of the MMP inhibitor. Following treatment with supernatant the suspension was washed with FACS buffer and cells were stained to identify HSPCs and CXCR4 expression. The following cocktail was used at 1:400 dilution for each antibody; lineage markers (CD45R, CD19, CD11b, CD3e, TER-119, CD2, CD8, CD4 and Ly6-C/G, all FITC positive) with antibodies against Sca1 and cKit to identify HSPCs (Lineage$^-$, Sca1$^+$, cKit$^+$). A CXCR4 antibody was used to determine the surface expression on HSPCs (as Geometric-Mean). Samples were run on the Fortessa X-20 and data were analysed using FlowJo (TreeStar).

**High performance liquid chromatography (HPLC) for Plasma Catecholamines:** Noradrenaline was extracted from plasma using alumina adsorption and was quantified using high performance liquid chromatography with coulometric detection as previously described.[31]

**Zymography:** To assess the effects of pressure on the gelatinase MMP9, gelatin zymography was performed on BM extracellular fluid, isolated by collecting the supernatant from flushed BM. Briefly, BM extracellular fluid samples were aliquoted on to 7.5% acrylamide, 0.5% gelatin gels and electrophoresed. Following electrophoresis, gels were washed and incubated overnight in incubation buffer at 37°C. 0.1% Coomassie Blue solution containing 40% 2-propanol was used to stain the gels. Further details can be found in the supplementary information.

**RNA isolation, cDNA synthesis and qRT-PCR:** Total RNA from BM cells was extracted using QIAGEN RNeasy mini kit and cDNA was synthesized using a Tetro cDNA kit (Bioline). qRT-PCR was assessed in real time with a 7500 Fast Real-Time PCR System (Applied Biosystems) using SYBR Green PCR Core Reagents (Agilent Technologies) and normalized to *GAPDH*. All primer sequences can be found in Supplementary Table 2.

**Statistics:** Data are presented as mean ± SEM (unless stated otherwise) and were analyzed using the two-tailed Student t-test or One-way ANOVA where appropriate. Analysis of baseline and final blood pressure between strains was analysed using a two-way ANOVA with the factors strain ($P_{strain}$) and time ($P_{time}$) followed by a Sidak post-hoc test to account for multiple

comparisons. A $P<0.05$ was considered significant. All tests were performed using the Prism software (GraphPad Software, Inc., La Jolla, CA).